

1 KIR gene content imputation from single-nucleotide
2 polymorphisms in the Finnish population

3 Jarmo Ritari^{1*}, Kati Hyvärinen¹, Jukka Partanen¹, Satu Koskela¹,

4 ¹Finnish Red Cross Blood Service, Helsinki, Finland

5 *Correspondence: jarmo.ritari@veripalvelu.fi; satu.koskela@veripalvelu.fi

6 Abstract

7 The killer cell immunoglobulin-like receptor (KIR) gene cluster on chromosome 19
8 encodes cell surface glycoproteins that bind class I human leukocyte antigen
9 (HLA) molecules as well as some other ligands. Through regulation of natural
10 killer (NK) cell activity KIRs participate in tumour surveillance and clearing viral
11 infections. KIR gene copy number variation associates with the outcome of
12 transplantations and susceptibility to immune-mediated diseases. Inferring KIR
13 gene content from genetic variant data is therefore desirable for immunogenetic
14 analysis, particularly in the context of growing biobank genome data collections
15 that rely on genotyping by microarray. Here we describe a stand-alone and freely
16 available gene content imputation for 12 KIR genes. The models were trained
17 using 818 Finnish biobank samples genotyped for 5774 KIR-region SNPs and
18 analysed for KIR gene content with targeted sequencing. Cross-validation results
19 demonstrate a high mean overall accuracy of 99.2% (95% CI: 97.8-99.7%) which
20 compares favourably with previous methods including short-read sequencing
21 based approaches.

22 Introduction

23 Killer cell immunoglobulin-like receptors (KIRs) regulate the activity of natural
24 killer (NK) cells and a subset of T cells via inhibitory and activating signals.
25 Through their KIR molecules NK cells detect phenotypic change in a target cell.
26 KIRs recognise human leukocyte antigen (HLA) class I molecules as cognate
27 ligands, limiting to particular HLA allotypes within the serological HLA-C1 and C2
28 allele groups (Wroblewski et al., 2019) HLA-Bw4 motif, HLA-A3/11, HLA-G and
29 HLA-F (Garcia-Beltran et al., 2016). The functional difference between inhibitory
30 and activating KIRs is determined by the presence or absence of a cytoplasmic
31 immunoreceptor tyrosine-based inhibitory (ITIM) protein motif, respectively. In
32 the absence of constitutive signaling conveyed by an inhibitory KIR binding to its
33 class I ligand, NK cell cytotoxic activity and cytokine production are triggered
34 (Lanier, 2008).

35 According to the missing-self hypothesis, NK cells recognise tumour or virally
36 infected cells that attempt to evade T cell mediated immunity by downregulating
37 their cell surface HLA-molecules that present intracellular antigens to T cells.

38 Activating KIRs, in contrast, are thought to recognise surface molecules
39 indicative of aberrant host cell activity such as an exceptionally high surface
40 density of HLA class I molecules even though in some cases the ligand remains
41 unknown (Ivarsson et al., 2014). Activating KIRs have lower affinity to their
42 ligands than inhibitory KIRs (Stewart et al., 2005) most likely owing to NK cell
43 education to maintain self-tolerance. However, upon receiving a sufficient
44 positive stimulus, they are able induce NK cell activation and target cell lysis. A
45 vast majority of genetic associations of KIRs with cancer, autoimmunity and
46 infectious diseases are attributed to variation in activating KIRs (Parham and
47 Guethlein, 2018).

48 The KIR gene cluster on the human chromosome 19q13.4 encodes fifteen
49 relatively homologous KIR genes and two pseudogenes, constituting two main
50 haplotypes: A and B (https://www.ebi.ac.uk/ipd/kir/sequenced_haplotypes.html).
51 The group A haplotype consists of functional *KIR3DL3*, *KIR2DL3*, *KIR2DL1*,
52 *KIR2DL4*, *KIR3DL1*, *KIR2DS4* and *KIR3DL2* genes of which all except *KIR2DS4* are
53 inhibitory. The group B haplotype, on the other hand, is more diverse being
54 characterised by the presence of at least one of *KIR2DS2*, *KIR2DL2*, *KIR2DL5*,
55 *KIR2DS5*, *KIR3DS1*, *KIR2DS3* or *KIR2DS1* genes (Bashirova et al., 2006). Thus, the
56 group B haplotype harbours several activating KIR genes, whereas the only
57 activating receptor, *KIR2DS4*, of the group A is in a significant proportion of
58 Caucasians a non-functional truncated variant (Bontadini et al., 2006; Maxwell et
59 al., 2002), rendering about 40% of group A homozygotes solely inhibitory.
60 Approximately 55% of haplotypes are mixtures between group A and B
61 (Middleton and Gonzelez, 2010), making the haplotype structure highly variable
62 in the population. Allelic diversity within KIRs is equally high with at least a few
63 hundred known polymorphisms (<https://www.ebi.ac.uk/ipd/kir/stats.html>), which
64 can affect class I ligand affinity (Carr et al., 2005; Frazier et al., 2013).

65 Discovery and interpretation of KIR gene and haplotype associations in large
66 biobank genome data collections can be facilitated by imputation of KIR content
67 from single-nucleotide polymorphisms (SNPs) genotyped by microarray.
68 Furthermore, in organ or stem cell transplantation setting the KIR locus offers
69 additional genetic information for donor selection and prediction of clinical
70 outcome (Cooley et al., 2010; Impola et al., 2014; Littera et al., 2017), and for
71 many of these clinical genome datasets SNP microarray provides the most cost-
72 effective genotyping platform as well. To date, several KIR copy number or gene
73 content analysis methods have been implemented for sequencing data (Chen et

74 al., 2020; Manianguou et al., 2017; Norman et al., 2016; Roe and Kuang, 2020;
75 Wagner et al., 2018), but to our knowledge only one SNP-based approach exists
76 so far (Vukcevic et al., 2015). These approaches reach a high accuracy which
77 makes KIR inference reliable enough for research and even practical clinical
78 applications. However, regarding biobank data, a stand-alone application that
79 does not require submitting individual genotype data to external servers would
80 be essential. To this end, we have implemented a random forest (RF) based KIR
81 gene content prediction in the R environment exploiting SNP data. The reference
82 data used for model fitting comprises KIR genotypes determined by targeted
83 sequencing and 5774 genotyped SNPs in the KIR chromosomal region. Based on
84 prediction of an independent subset of data, our results demonstrate a mean
85 overall accuracy of 99.2% which is comparable to previously published methods.

86 [Materials and Methods](#)

87 [Subjects](#)

88 Genomic DNA samples from blood donors and their genotypes were obtained
89 from the Blood Service Biobank, Helsinki, Finland. The samples were collected
90 from Finnish blood donors who had given a broad biobank consent according to
91 the Finnish Biobank Act (688/2012).

92 [Genotyping](#)

93 Genotyping of samples was originally performed on a customized ThermoFisher
94 Axiom array at the Thermo Fisher genotyping service facility (San Diego, USA) as
95 a part of the FinnGen project. After the embargo period, the genotypes were
96 returned to the Blood Service Biobank.

97 Genotype calling and quality control steps are described in
98 finngen.gitbook.io/documentation/methods/genotype-imputation. The array
99 markes files can be downloaded from www.finnngen.fi/en/researchers/genotyping.
100 The protocol for genotype data liftover to hg38/GRCh38 is described in detail in
101 [www.protocols.io/view/genotyping-chip-data-lift-over-to-reference-genome-](https://www.protocols.io/view/genotyping-chip-data-lift-over-to-reference-genome-xbhfj6?version_warning=no)
102 [xbhfj6?version_warning=no](https://www.protocols.io/view/genotyping-chip-data-lift-over-to-reference-genome-xbhfj6?version_warning=no), and genotype imputation protocol is described in
103 www.protocols.io/view/genotype-imputation-workflow-v3-0-xbgfijw. KIR

104 genotyping at absence-presence level of 818 samples was purchased from
105 Histogenetics LLC (NY, USA).

106 Imputation models

107 The outline of the modelling set up is depicted in Figure 1. The random forest
108 model for predicting KIR gene content was implemented with R v4.0.4 (R Core
109 Team, 2021) using the library ranger v0.12.1 (Wright and Ziegler, 2017). The
110 model error was estimated by dividing the data randomly into two equal subsets
111 to one of which a RF model for each KIR gene was fitted while the other subset
112 was used for prediction with the fitted model. SNP dosage values in the KIR
113 region on chr19 were used as predictor variables, and the KIR gene content (1
114 for presence, 0 for absence) as determined by targeted sequencing served as
115 the target phenotype variable. Feature selection within the model fitting was
116 implemented using the permuted importance metric. Variants achieving an
117 importance $>1 \times 10^{-5}$ were accepted into the model. The final model was fitted
118 with the full dataset (Figure 1).

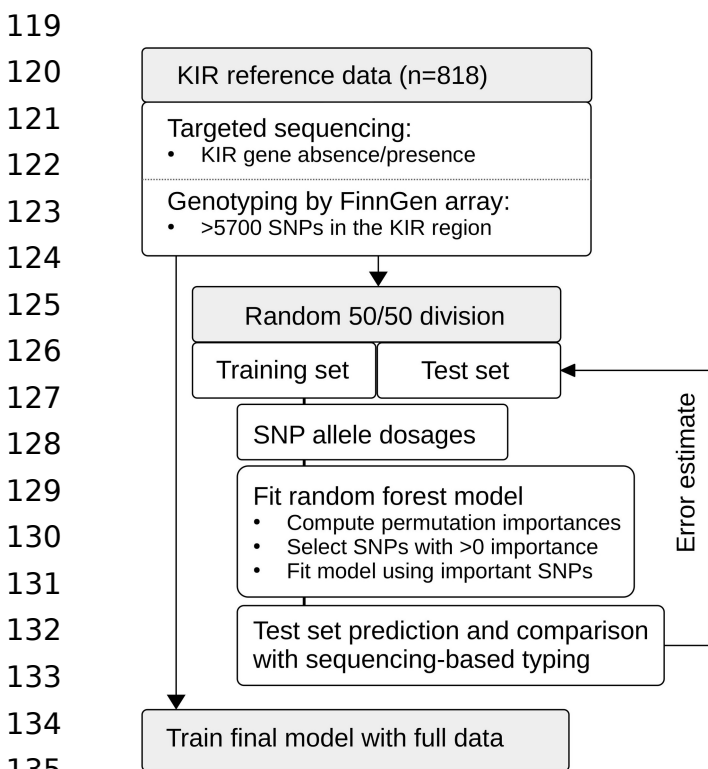


Figure 1. Schematic presentation of the study setup. The reference data set of 818 individuals was genotyped on the FinnGen SNP array, and KIR gene content was determined by targeted sequencing. We used random forests to fit models to the training data set comprising randomly selected 409 individuals. Feature selection was based on the importance metric computed through permutation. The model was re.fitted on SNPs achieving an importance of >0 . Based on the test set comprising the other half of the samples, we calculated prediction error estimates for the modeling approach. Finally, we used the whole data set to train complete models.

136 Accuracy metrics were calculated using the R library caret v6.0-86 (Kuhn, Max,
137 2020). Positive predictive value (PPV) was defined as (sensitivity * prevalence) /

138 $((\text{sensitivity} \times \text{prevalence}) + ((1 - \text{specificity}) \times (1 - \text{prevalence})))$. Negative predictive
139 value (NPV) was defined as $(\text{specificity} \times (1 - \text{prevalence})) / (((1 -$
140 $\text{sensitivity}) \times \text{prevalence}) + ((\text{specificity}) \times (1 - \text{prevalence})))$. Balanced accuracy was
141 calculated as $(\text{sensitivity} + \text{specificity}) / 2$. Overall accuracy was calculated as the
142 proportion of correct calls from all calls with 95% confidence intervals
143 determined by binomial distribution. The data were managed with the tidyverse
144 v1.3.0 (Wickham et al., 2019) package system.

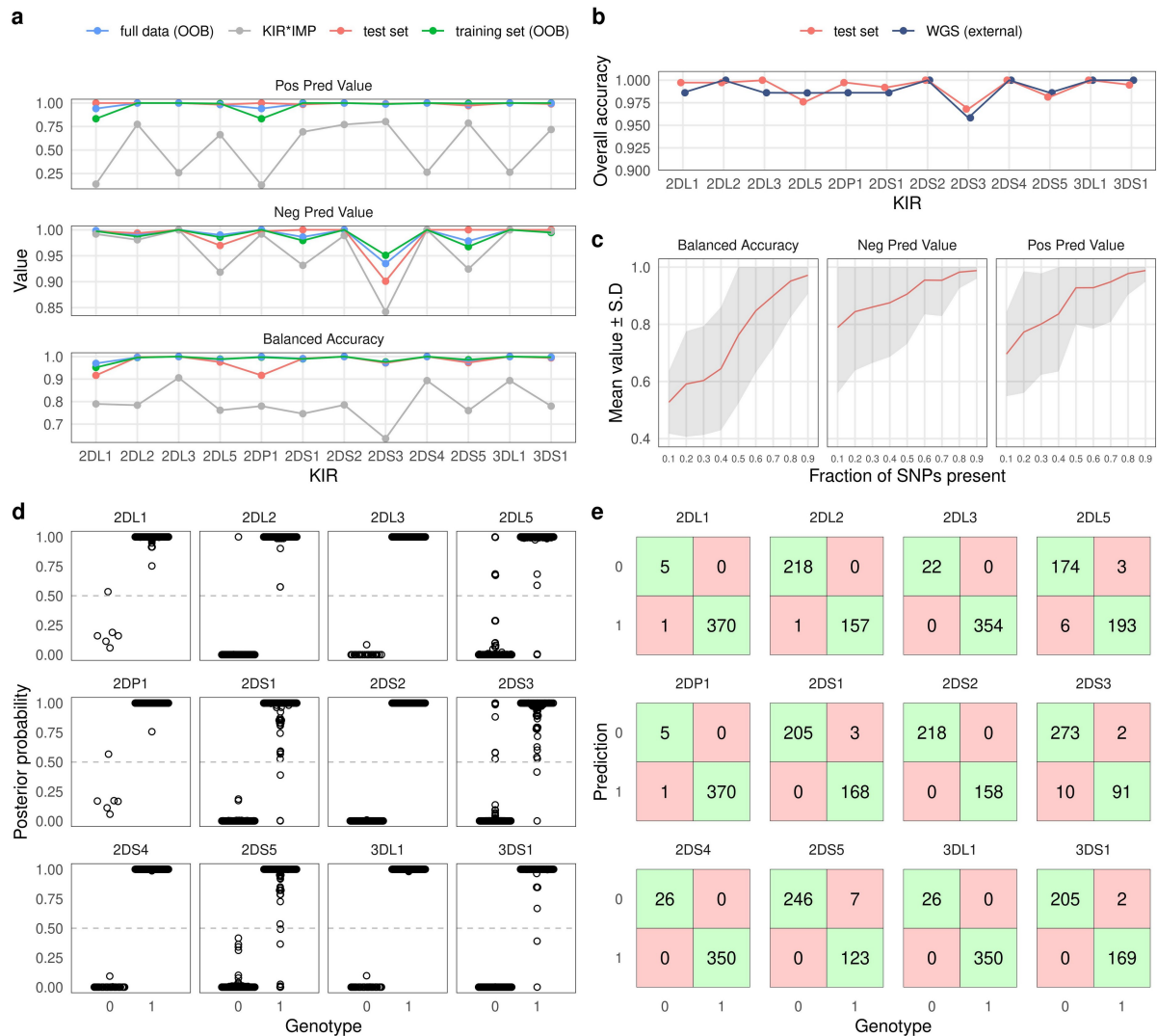
145 To compare our method with KIR*IMP, KIR*IMP v1.2.0
146 (<http://imp.science.unimelb.edu.au/kir/>) (Vukcevic et al., 2015) was applied to
147 the 818 samples constituting our reference panel. Prior to submitting the data to
148 KIR*IMP, the genotypes were transferred to hg19 coordinates with UCSC LiftOver
149 (<http://genome.ucsc.edu/cgi-bin/hgLiftOver>) and phased with shapeit v2.r904
150 (O'Connell et al., 2014) with default parameters except for burn=10, prune=10,
151 main=50 and window=0.5. The orientations of the SNPs in the phased dataset
152 were harmonised according to the KIR*IMP SNP information file
153 (<http://imp.science.unimelb.edu.au/kir/static/kirimp.uk1.snp.info.csv>) using a
154 custom R script. In analysing the results, we used KIR2DS4TOTAL and
155 KIR3DL1ex9 CNV imputation results of KIR*IMP to compare with our KIR2DS4 and
156 KIR3DL1 absence-presence imputations, respectively.

157 Code availability

158 The analysis code and the models are available at [https://github.com/FRCBS/KIR-](https://github.com/FRCBS/KIR-imputation)
159 [imputation](https://github.com/FRCBS/KIR-imputation).

160 Results

161 Accuracy estimates for each KIR gene for prediction of an independent test set
162 are listed in Table 1. In summary, the mean overall accuracy of prediction was
163 0.992 (95% CI 0.997–0.978). The lowest accuracy of 0.968 (95% CI 0.983–0.945)
164 was obtained for KIR2DS3 while KIR2DL3, KIR2DS2, KIR2DS4 and KIR3DL1 all
165 achieved an overall accuracy of 1. Accuracy estimates for the test data and the
166 RF out-of-bag (training set and full data) are plotted in Figure 2a. SNPs used by
167 the models are listed in Supplementary Table 1.



168 **Figure 2.** Overview of KIR prediction accuracy. **a)** Prediction performance metrics for the
 169 12 imputed KIR genes. OOB: out-of-bag estimate from random forest models. Test set
 170 was predicted by models fitted on the training set. KIR*IMP was applied to the full
 171 dataset. Note the varying scale of the y-axis. **b)** Comparison of overall accuracies
 172 between the test set and reported values for the WGS based method kpi extracted from
 173 the publication by Chen and co-workers. **c)** Impact of missing SNPs on prediction
 174 performance in the test set. **d)** Posterior probability distributions for test set prediction.
 175 Genotypes 0 and 1 denote absence and presence of a KIR gene, respectively. **e)**
 176 Confusion tables for the test set prediction. Posterior probabilities >0.5 were classified as
 177 'present'.

178 To compare our approach with KIR*IMP, we converted our dataset of 818
 179 samples to hg19 genome build and harmonised the SNP orientations. 126 SNPs
 180 out of 5774 could not be lifted over to hg19, and out of the 301 SNPs used by
 181 KIR*IMP 249 were found in our input data. SNP allele frequencies between the
 182 KIR*IMP reference panel and the input data had Pearson's correlation coefficient

183 of 0.968 (Supplementary Figure 1a). Mean accuracy based on an estimate from
 184 the KIR*IMP reference subsetting for the input SNPs was 96.59% (Supplementary
 185 Figure 1b). Accuracy metrics for the imputation of our data by KIR*IMP are
 186 indicated by grey colour in Figure 2a. In summary, for all 12 included KIR genes
 187 we observed a distinctly lower imputation accuracy for KIR*IMP in comparison
 188 with our method.

189 **Table 1.** KIR imputation accuracy.

| KIR_gene | Sensitivity | Specificity | Pos. Pred. Value | Neg. Pred. Value | Precision | Recall | Balanced accuracy | Overall accuracy |
|----------|-------------|-------------|------------------|------------------|-----------|--------|-------------------|------------------|
| 2DL1 | 0.833 | 1 | 1 | 0.997 | 1 | 0.833 | 0.917 | 0.997 |
| 2DL2 | 0.995 | 1 | 1 | 0.994 | 1 | 0.995 | 0.998 | 0.997 |
| 2DL3 | 1 | 1 | 1 | 1 | 1 | 1 | 1 | 1 |
| 2DL5 | 0.967 | 0.985 | 0.983 | 0.97 | 0.983 | 0.967 | 0.976 | 0.976 |
| 2DP1 | 0.833 | 1 | 1 | 0.997 | 1 | 0.833 | 0.917 | 0.997 |
| 2DS1 | 1 | 0.982 | 0.986 | 1 | 0.986 | 1 | 0.991 | 0.992 |
| 2DS2 | 1 | 1 | 1 | 1 | 1 | 1 | 1 | 1 |
| 2DS3 | 0.965 | 0.978 | 0.993 | 0.901 | 0.993 | 0.965 | 0.972 | 0.968 |
| 2DS4 | 1 | 1 | 1 | 1 | 1 | 1 | 1 | 1 |
| 2DS5 | 1 | 0.946 | 0.972 | 1 | 0.972 | 1 | 0.973 | 0.981 |
| 3DL1 | 1 | 1 | 1 | 1 | 1 | 1 | 1 | 1 |
| 3DS1 | 1 | 0.988 | 0.99 | 1 | 0.99 | 1 | 0.994 | 0.995 |

190 To compare the level of overall accuracy of our SNP-based method with an
 191 established sequencing-based approach, we extracted the results of the
 192 evaluation by Chen and coworkers (Chen et al., 2020) for the KIR imputation
 193 method kpi (Roe and Kuang, 2020). Figure 2b shows the accuracy of kpi
 194 compared with our test set results. The observed values were highly similar with
 195 KIR2DS3 being the most difficult gene to impute correctly.

196 Varying numbers of missing SNPs within the KIR region reduced the imputation
 197 accuracy in accordance with the fraction of removed variants. At 80% of the
 198 SNPs present the accuracy generally remained at a good level but started to
 199 increasingly deteriorate after that (Figure 2c).

200 Posterior probability (PP) values of imputation are informative of imputation
 201 uncertainty and can be incorporated into association analyses (Zhou et al.,
 202 2020). Figure 2d shows the PP distributions for each imputed KIR gene.
 203 Classification performances according to the PP threshold where PPs below 0.5
 204 were classified as a missing KIR gene are shown by confusion tables in Figure 2e.
 205 KIR genes with a higher error rate typically exhibited a PP distribution indicative
 206 of higher uncertainty as more values were closer to 0.5 than 1 or 0.

207 Discussion

208 Genome data generated in a growing number of biobank projects is instrumental
209 to detailed immunogenetic analyses of several clinical phenotypes and diseases.
210 Within the current technological and economical constraints SNP microarrays
211 offer a practical way for genotyping hundreds of thousands of individuals. The
212 KIR gene content, despite being a relatively coarse-scale feature, has been
213 shown to influence many immune-mediated disorders (Bashirova et al., 2006;
214 Parham and Guethlein, 2018) and complications in pregnancy (Colucci, 2017).
215 Imputation of KIR gene content from SNPs in a scalable way is therefore essential
216 to analysing and interpreting large biomedical databases. To this end, in the
217 present study we have built a machine learning model for inferring KIR gene
218 content from SNP dosage data for stand-alone application in biobanks and other
219 clinical data collections. Exploitation of random forest for imputing KIRs from SNP
220 genotypes was first implemented in the KIR*IMP software (Vukcevic et al., 2015),
221 which runs on a remote server (<http://imp.science.unimelb.edu.au/kir/>). The main
222 difference of our method in comparison with KIR*IMP is that it does not require
223 phased data and the models can be downloaded and run locally. However,
224 KIR*IMP produces a more detailed output that includes A and B haplotypes,
225 framework genes KIR3DP1 and KIR2DL4, variants of KIR2DS4 and KIR3DL1 and
226 gene copy numbers. Otherwise, at the level of gene absence-presence, the
227 imputation accuracy of our method compares favourably not only with KIR*IMP
228 but also to sequencing-based methods (Chen et al., 2020; Roe and Kuang, 2020).

229 In all imputation evaluations KIR2DS3 demonstrated the largest error in overall
230 accuracy, followed by KIR2DL5 and KIR2DS5. A common feature shared by these
231 three genes is that their location within the KIR chromosomal region is not fixed
232 but can vary between centromeric and telomeric positions (Hsu et al., 2002; Pyo
233 et al., 2010). Conceivably, this kind of positional variance may confound the
234 identification of predictive SNPs resulting in greater imputation uncertainty.
235 Other challenging genes were KIR2DL1 and KIR2DP1 which both harbour a
236 relatively rare gene absence with population frequency of about 1.6%, and
237 therefore had few cases in the training data. In this regard, the out-of-bag
238 estimate for the whole dataset might be the most reliable error estimate for
239 these genes, suggesting a balanced accuracy and positive predictive value of
240 about 0.95. Despite some challenges, KIR gene content imputation presents a

241 valuable tool for initial screening and provides a rational basis for further
242 analyses.

243 Allelic diversity, copy number variation and homologous gene sequences make
244 KIR typing challenging by NGS or microarray probes. Nevertheless, the large
245 number of variants within the region allows extraction of information based on
246 linkage with gene content, even if the causative variants cannot in all cases be
247 directly measured. This is also a shortcoming because linkage patterns vary
248 between populations and consequently models trained on one population may
249 not be fully transferrable to another. While the informative SNPs used by our
250 method are not specific to the Finnish population as such, but present a set of
251 common genetic variants with relatively similar allele frequencies across
252 European populations, it is not guaranteed that the prediction would achieve as
253 good an accuracy in populations other than Finns. Our method is also limited by
254 the requirement of the availability of informative SNPs in the dataset under
255 analysis. These variants are not genotyped by all microarrays commonly used in
256 genome analysis and therefore selection of a suitable platform is crucial. Another
257 noteworthy limitation is that the method is not capable of identifying alleles. To
258 date, only targeted sequencing based approaches can resolve KIR alleles
259 (Maniangou et al., 2017; Norman et al., 2016; Roe and Kuang, 2020; Wagner et
260 al., 2018). A possible future direction therefore is to extend KIR imputation from
261 SNPs to cover allelic diversity.

262 [Acknowledgements](#)

263 The study was supported by the Academy of Finland, the Finnish Cancer
264 Association, VTR funding from the Finnish Government, and Business Finland.
265 The funders and biobanks had no role in study design, data collection and
266 analysis, decision to publish, or preparation of the manuscript. We thank the
267 Finnish Red Cross Blood Service Biobank and the blood donors for providing the
268 samples. FinnGen is acknowledged for providing the SNP genotype data.

269 [Competing interests](#)

270 The authors declare no competing interests.

271 References

- Bashirova AA, Martin MP, McVicar DW, Carrington M. 2006. The Killer Immunoglobulin-Like Receptor Gene Cluster: Tuning the Genome for Defense. *Annu Rev Genom Hum Genet* **7**:277–300. doi:10.1146/annurev.genom.7.080505.115726
- Bontadini A, Testi M, Cuccia M, Martinetti M, Carcassi C, Chiesa A, Cosentini E, Dametto E, Frison S, Iannone A, Lombardo C, Malagoli A, Mariani M, Mariotti L, Mascaretti L, Mele L, Miotti V, Nesci S, Ozzella G, Piantatelli D, Romeo G, Tagliaferri C, Vatta S, Andreani M, Conte R. 2006. Distribution of killer cell immunoglobulin-like receptors genes in the Italian Caucasian population. *J Transl Med* **4**:44. doi:10.1186/1479-5876-4-44
- Carr WH, Pando MJ, Parham P. 2005. KIR3DL1 Polymorphisms That Affect NK Cell Inhibition by HLA-Bw4 Ligand. *J Immunol* **175**:5222–5229. doi:10.4049/jimmunol.175.8.5222
- Chen J, Madireddi S, Nagarkar D, Migdal M, Vander Heiden J, Chang D, Mukhyala K, Selvaraj S, Kadel EE, Brauer MJ, Mariathasan S, Hunkapiller J, Jhunhunwala S, Albert ML, Hammer C. 2020. In silico tools for accurate HLA and KIR inference from clinical sequencing data empower immunogenetics on individual-patient and population scales. *Briefings in Bioinformatics* bbaa223. doi:10.1093/bib/bbaa223
- Colucci F. 2017. The role of KIR and HLA interactions in pregnancy complications. *Immunogenetics* **69**:557–565. doi:10.1007/s00251-017-1003-9
- Cooley S, Weisdorf DJ, Guethlein LA, Klein JP, Wang T, Le CT, Marsh SGE, Geraghty D, Spellman S, Haagenson MD, Ladner M, Trachtenberg E, Parham P, Miller JS. 2010. Donor selection for natural killer cell receptor genes leads to superior survival after unrelated transplantation for acute myelogenous leukemia. *Blood* **116**:2411–2419. doi:10.1182/blood-2010-05-283051
- Frazier WR, Steiner N, Hou L, Dakshanamurthy S, Hurley CK. 2013. Allelic Variation in KIR2DL3 Generates a KIR2DL2-like Receptor with Increased Binding to its HLA-C Ligand. *Jl* **190**:6198–6208. doi:10.4049/jimmunol.1300464
- Garcia-Beltran WF, Hölzemer A, Martrus G, Chung AW, Pacheco Y, Simoneau CR, Rucevic M, Lamothe-Molina PA, Pertel T, Kim T-E, Dugan H, Alter G, Dechanet-Merville J, Jost S, Carrington M, Altfeld M. 2016. Open conformers of HLA-F are high-affinity ligands of the activating NK-cell receptor KIR3DS1. *Nat Immunol* **17**:1067–1074. doi:10.1038/ni.3513
- Hsu KC, Chida S, Geraghty DE, Dupont B. 2002. The killer cell immunoglobulin-like receptor (KIR) genomic region: gene-order, haplotypes and allelic polymorphism: Hsu et al · KIR genomic region and KIR haplotypes. *Immunological Reviews* **190**:40–52. doi:10.1034/j.1600-065X.2002.19004.x
- Impola U, Turpeinen H, Alakulppi N, Linjama T, Volin L, Niittyvuopio R, Partanen J, Koskela S. 2014. Donor Haplotype B of NK KIR Receptor Reduces the Relapse Risk in HLA-Identical Sibling Hematopoietic Stem Cell Transplantation of AML Patients. *Front Immunol* **5**. doi:10.3389/fimmu.2014.00405
- Ivarsson MA, MichaÅ«lsson J, Fauriat C. 2014. Activating Killer Cell Ig-Like Receptors in Health and Disease. *Front Immunol* **5**. doi:10.3389/fimmu.2014.00184
- Kuhn, Max. 2020. caret: Classification and Regression Training.

- Lanier LL. 2008. Up on the tightrope: natural killer cell activation and inhibition. *Nat Immunol* **9**:495–502. doi:10.1038/ni1581
- Littera R, Piredda G, Argiolas D, Lai S, Congeddu E, Ragatzu P, Melis M, Carta E, Michittu MB, Valentini D, Cappai L, Porcella R, Alba F, Serra M, Loi V, Maddi R, Orrù S, La Nasa G, Caocci G, Cusano R, Arras M, Frongia M, Pani A, Carcassi C. 2017. KIR and their HLA Class I ligands: Two more pieces towards completing the puzzle of chronic rejection and graft loss in kidney transplantation. *PLoS ONE* **12**:e0180831. doi:10.1371/journal.pone.0180831
- Maniangou B, Legrand N, Alizadeh M, Guyet U, Willem C, David G, Charpentier E, Walencik A, Retière C, Gagne K. 2017. Killer Immunoglobulin-Like Receptor Allele Determination Using Next-Generation Sequencing Technology. *Front Immunol* **8**:547. doi:10.3389/fimmu.2017.00547
- Maxwell LD, Wallace A, Middleton D, Curran MD. 2002. A common KIR2DS4 deletion variant in the human that predicts a soluble KIR molecule analogous to the KIR1D molecule observed in the rhesus monkey: Maxwell et al: A predicted soluble KIR2DS4 deletion variant. *Tissue Antigens* **60**:254–258. doi:10.1034/j.1399-0039.2002.600307.x
- Middleton D, Gonzelez F. 2010. The extensive polymorphism of KIR genes. *Immunology* **129**:8–19. doi:10.1111/j.1365-2567.2009.03208.x
- Norman PJ, Hollenbach JA, Nemat-Gorgani N, Marin WM, Norberg SJ, Ashouri E, Jayaraman J, Wroblewski EE, Trowsdale J, Rajalingam R, Oksenberg JR, Chiaroni J, Guethlein LA, Traherne JA, Ronaghi M, Parham P. 2016. Defining KIR and HLA Class I Genotypes at Highest Resolution via High-Throughput Sequencing. *The American Journal of Human Genetics* **99**:375–391. doi:10.1016/j.ajhg.2016.06.023
- O’Connell J, Gurdasani D, Delaneau O, Pirastu N, Ulivi S, Cocca M, Traglia M, Huang J, Huffman JE, Rudan I, McQuillan R, Fraser RM, Campbell H, Polasek O, Asiki G, Ekoru K, Hayward C, Wright AF, Vitart V, Navarro P, Zagury J-F, Wilson JF, Toniolo D, Gasparini P, Soranzo N, Sandhu MS, Marchini J. 2014. A General Approach for Haplotype Phasing across the Full Spectrum of Relatedness. *PLoS Genet* **10**:e1004234. doi:10.1371/journal.pgen.1004234
- Parham P, Guethlein LA. 2018. Genetics of Natural Killer Cells in Human Health, Disease, and Survival. *Annu Rev Immunol* **36**:519–548. doi:10.1146/annurev-immunol-042617-053149
- Pyo C-W, Guethlein LA, Vu Q, Wang R, Abi-Rached L, Norman PJ, Marsh SGE, Miller JS, Parham P, Geraghty DE. 2010. Different Patterns of Evolution in the Centromeric and Telomeric Regions of Group A and B Haplotypes of the Human Killer Cell Ig-Like Receptor Locus. *PLoS ONE* **5**:e15115. doi:10.1371/journal.pone.0015115
- R Core Team. 2021. R: A language and environment for statistical computing. Vienna, Austria: R Foundation for Statistical Computing.
- Roe D, Kuang R. 2020. Accurate and Efficient KIR Gene and Haplotype Inference From Genome Sequencing Reads With Novel K-mer Signatures. *Front Immunol* **11**:583013. doi:10.3389/fimmu.2020.583013
- Stewart CA, Laugier-Anfossi F, Vely F, Saulquin X, Riedmuller J, Tisserant A, Gauthier L, Romagne F, Ferracci G, Arosa FA, Moretta A, Sun PD, Ugolini S, Vivier E. 2005. Recognition of peptide-MHC class I complexes by activating killer immunoglobulin-like receptors. *Proceedings of the National Academy of Sciences* **102**:13224–13229. doi:10.1073/pnas.0503594102
- Vukcevic D, Traherne JA, Næss S, Ellinghaus E, Kamatani Y, Dilthey A, Lathrop M, Karlsen TH, Franke A, Moffatt M, Cookson W, Trowsdale J, McVean G, Sawcer S, Leslie S. 2015. Imputation of KIR Types from SNP Variation Data. *The American Journal of Human Genetics* **97**:593–607. doi:10.1016/j.ajhg.2015.09.005

- Wagner I, Schefzyk D, Pruschke J, Schöfl G, Schöne B, Gruber N, Lang K, Hofmann J, Gnahn C, Heyn B, Marin WM, Dandekar R, Hollenbach JA, Schetelig J, Pingel J, Norman PJ, Sauter J, Schmidt AH, Lange V. 2018. Allele-Level KIR Genotyping of More Than a Million Samples: Workflow, Algorithm, and Observations. *Front Immunol* **9**:2843. doi:10.3389/fimmu.2018.02843
- Wickham H, Averick M, Bryan J, Chang W, McGowan L, François R, Golemund G, Hayes A, Henry L, Hester J, Kuhn M, Pedersen T, Miller E, Bache S, Müller K, Ooms J, Robinson D, Seidel D, Spinu V, Takahashi K, Vaughan D, Wilke C, Woo K, Yutani H. 2019. Welcome to the Tidyverse. *JOSS* **4**:1686. doi:10.21105/joss.01686
- Wright MN, Ziegler A. 2017. ranger : A Fast Implementation of Random Forests for High Dimensional Data in C++ and R. *J Stat Soft* **77**. doi:10.18637/jss.v077.i01
- Wroblewski EE, Parham P, Guethlein LA. 2019. Two to Tango: Co-evolution of Hominid Natural Killer Cell Receptors and MHC. *Front Immunol* **10**:177. doi:10.3389/fimmu.2019.00177
- Zhou W, Zhao Z, Nielsen JB, Fritsche LG, LeFaive J, Gagliano Taliun SA, Bi W, Gabrielsen ME, Daly MJ, Neale BM, Hveem K, Abecasis GR, Willer CJ, Lee S. 2020. Scalable generalized linear mixed model for region-based association tests in large biobanks and cohorts. *Nat Genet* **52**:634–639. doi:10.1038/s41588-020-0621-6